Cumhuriyet Sci. J., 44(4) (2023) 793-798
DOI: https://doi.org/10.17776/csj.1349975

Cumhuriyet Science Journal

| csj.cumhuriyet.edu.tr | Founded: 2002 ISSN: 2587-2680 e-ISSN: 2587-246X Publisher: Sivas Cumhuriyet University

A Study on The Optical Properties of Long-Infrared Intraband Transitions of Quadruple Gaas/$Al_xga_{1-x}as$ Quantum Well Under Applied Electric Field

Didem Altun[1,a,*]

[1] *Sivas Vocational College, Sivas Cumhuriyet University, 58140, Sivas, Türkiye.*

**Corresponding author*

Research Article

History
Received: 25/08/2023
Accepted: 05/12/2023

ABSTRACT

Semiconductor-emitting/absorbing infrared devices are in the common interest of the scientific and industrial community due to their broad application in these fields. GaAs/AlGaAs based devices are one of the most studied semiconductor heterostructures. In this study, I have aimed to design GaAs/AlGaAs quantum well (QW) semiconductor heterostructures to emit/absorb in the long-infrared region and studied the optical properties. To do that, I have designed a quadruple QW, which is composed of GaAs/$Al_{0.44}Ga_{0.56}As$ QW and quantum barriers (QB). I have solved the time-independent Schrödinger equation using the finite element method-based matlab code under effective mass approximation. The wave functions and corresponding energy eigenvalues are obtained for varied electric field (EF) intensities. I have shown that our design can operate up to $80\ kV/cm$, which is the limit for first bounded energy eigenstates. It is observed that E_{32} transition provides long-infrared emission/absorption corresponding to the $0.12 - 0.14\ eV$ transition energy and it is constant with increased EF intensity. In addition, it is seen that the overlap of the wave functions is increasing with EF intensity which enhances radiative transition in the structure. I have calculated the linear absorption coefficient and refractive index change. I have observed that the absorption coefficient of E_{32} transition is increasing with EF intensity while E_{31} is decreasing and E_{21} is constant. As a last, I have shown that EF intensity has a minor effect on refractive index change.

Keywords: GaAs/$Al_{0.44}Ga_{0.56}As$, Optical properties, Absorption coefficient, Refractive index.

[a] *didemaltun@cumhuriyet.edu.tr* *https://orcid.org/0000-0002-1964-3538*

Introduction

Infrared light sources have been given attention in industry, health, and military applications due to the long-range transmission and high coherence of the electromagnetic source in the last couple of decades [1]. The infrared sensors have found space in target tracking, missile guiding, and night vision [2]. In addition, the infrared sensors are also widely used in telecommunication and health applications with a lower cost of production [3]. One of the most used infrared light sources is mercury-based materials but difficulties in production make working with these materials reluctant [4]. Beyond the Mercury-based materials, infrared light sources are rare, and the device performances are not the best till now. Because of that, low-dimensional GaAs-based materials are an option, and multi-quantum well structures have become very attractive for infrared devices. These material groups not only offer an option for the infrared sensor, but it has also made it possible to produce a device that emits infrared light. Due to the superior performances of the light emitting property of the GaAs-based materials, GaAs/AlGaAs multiple quantum wells have been widely used as the infrared laser source.

The electron transitions, in the quantum wells, between the bands and minibands emit/absorb infrared light [5]. For wider material selection, intra-band transition, which uses the space within the band, is used, unlike inter-band transition. An extensive study of intraband infrared transitions has been done by Hao. [6]. The wavelength of the device is set by tuning the quantum well width and barrier thicknesses. In these light sources, GaAs and AlGaAs materials are frequently used due to negligible lattice constant difference which makes wavelength control of the device easier. Furthermore, the relatively easier growth of the GaAs materials than other materials is another advantage of these materials [7].

Beyond the advantage of the material property, the reaction of the GaAs-based low-dimensional structures to the external fields has shown superior performance. These structures are mostly used as a light sources and are mostly electrical pumped so that there is no any external light source to trigger nonlinear properties. In addition to this, importance of electric filed is shown up here as a pump source. The electric field, magnetic field, temperature, pressure, and laser field have been applied to the GaAs-based quantum wells. In these studies, optical and electronic properties have been studied by many researchers [8-12]. In the study conducted by Öztürk, linear optical properties of GaAs/AlGaAs OWs were calculated depending on the applied electric field, and changes were observed in the potential profile shape, energy levels and dipole moments. This has shown that

the variation of resonance peaks suitable for optical modulators and infrared optical device applications can be achieved smoothly by changing the electric field [13].In addition; the effect of the laser field on the optical properties of the asymmetric quantum well has been analyzed [14]. Pöschl–Teller potential has been studied to analyze nonlinear optical properties [15]. The effect of the temperature and hydrostatic pressure on the optical and electronic properties has been studied by Öztürk [16]. The effects of the quantum well and barrier thicknesses have been investigated by Alaydin [17]. The electric and magnetic field effects applied to the QW structure with increasing well widths were shown by Altun [18].

In this report, I have considered energy band structures of long-infrared emitting/absorbing GaAs/$Al_xGa_{1-x}As$ quadruple quantum well heterojunction structures under varying EF for quantum cascade laser/detector applications. The wave functions and the corresponding energy eigenvalues have been obtained by solving the Schrödinger equation using effective mass approximation. The finite element method is used to obtain solutions. The EF intensity has been applied through positive growth direction and the intensity of the EF changes from $0-80\ kV/cm$ to analyze the optical properties of the structure under real device operation conditions. The three bounded energy states are obtained and the probability density of wave functions (PDW), transitions energies, and dipole moment matrix elements (DMME) are first calculated. Then, the changes in the linear refractive indices and absorption coefficients depending on the EF are investigated to be used in long-infrared devices.

Materials and Methods

In this research, GaAs/$Al_{0.44}Ga_{0.56}As$ quadruple quantum well heterojunction grown in z-direction is studied. QW structure is designed to obtain long-infrared transition between subbands. The details of the calculation methods are very well known in the literature and given by the references Altun, [18], Alaydin [19]. The EF is set perpendicular to the growth surface as $\vec{F} = F\hat{z}$. Hamiltonian with an external field (electric field) is defined as [17];

$$H = -\frac{\hbar^2}{2m^*}\frac{d^2}{dz^2} + V(z) + eFz \qquad (1)$$

In equation (1), m^* describes the effective mass of the electron in GaAs and in this research, it is taken as $m^* = 0.067m_0$ (m_0 is the free electron mass), e is the electron charge and $V(z)$ is the confinement potential. For GaAs/$Al_{0.44}Ga_{0.56}As$ system conduction band offset is taken as 0.6 and potential discontinuity $V(z)$ is 448 meV. V(z) potential height is the same as the reference [20]. Where the second-order differential is defined as;

$$\frac{d^2}{dz^2} = \left[-2\,diag\big(ones(1,N)\big) + diag(ones(1,N-1),-1) + diag(ones(1,N-1),1)\right]^2 \qquad (2)$$

N is the length of the matrix to define the total quantum region. After obtaining the energy levels and wave functions, linear absorption coefficient is calculated as follows [21]:

$$\beta(w) = w\sqrt{\frac{\mu}{\varepsilon_r}}\frac{|M_{ij}|^2\sigma_v\hbar\Gamma_{ij}}{(\Delta E_{ij}-\hbar w)^2+(\hbar\Gamma_{ij})^2} \qquad (3)$$

where w is the angular frequency, Γ_{ij} is the intersubband relaxation time, μ is the magnetic permeability, ε_r is the real part of the electrical permittivity, σ_v is the carrier number, $\hbar$ is the reduced Planck constant and ΔE_{ij} is the energy difference between final and initial energy levels of the electron. M_{ij} is the dipole matrix element and it is defined as [22];

$$M_{ij} = \int \psi_j(z)^*\,|e|\,z\,\psi_i(z)\,dz \qquad (4)$$

The linear refractive index change is expressed as [23]:

$$\frac{\Delta n(w)}{n_r} = \frac{|M_{ij}|^2\sigma_v}{2n_r^2\varepsilon_0}\left[\frac{\Delta E_{ij}-\hbar w}{(\Delta E_{ij}-\hbar w)^2+(\hbar\Gamma_{ij})^2}\right] \qquad (5)$$

Results and discussion

In this study, I analyze GaAs/$Al_xGa_{1-x}As$ quadruple QW structures to have long-infrared emission/absorption. To reach long-infrared wavelength (THz region), aluminum concentration is set to 0.44, which is the border of direct to indirect bandgap transition and $Al_{0.45}Ga_{0.55}As$ has a direct bandgap [20]. The potential barrier height of the QW is calculated as $V_0 = 448\ meV$ and the thickness of the layer sequence of quadruple QW heterostructures is as follows **8**-2.2-**1.2**-2-**1**-4-**2.3**-1.2-**8** nm (QB are shown bold). The effective mass approximation is used to solve the Schrödinger equation using the finite element method (FEM) and the parameters used in this study are $\mu = 4\pi\,x10^{-7}\,H/m$, $\sigma = 1x10^{22}\,cm^{-3}$, $\tau_{21} = 0.3\,ps$, $\tau_{32} = 2.8\,ps$, and $\tau_{31} = 4\,ps$, $\Gamma_{ij} = \frac{1}{\tau_{ij}}$ and $n_r = 3.3254$.

In the calculations, I have seen that there are only three bounded states and I have considered carrier transitions in these states as shown in Figure 1.

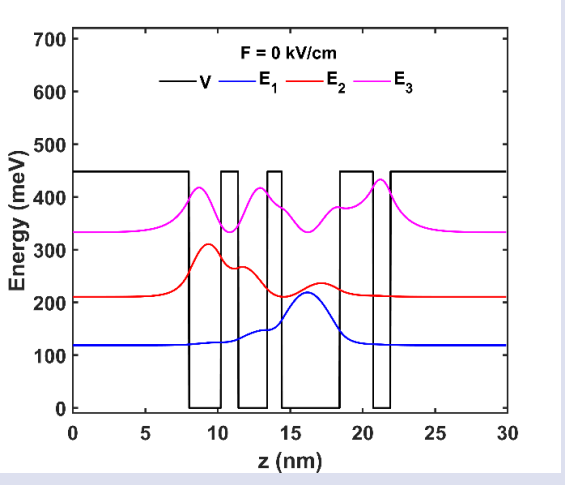

Figure 1. PDW of quadruple QW structure in the absence of EF.

In the case of zero EF, the ground state is mostly localized in the third (from left to right) QW. While the first excited state is mostly localized in the first QW, its localization has been distributed up to the end of the second QW. Apart from the ground and first excited state the second excited state's localization has been distributed between the first, second, and fourth QWs. As seen in Figure 1, energy eigenvalues of the ground, first excited, and second excited states are as follows $119\ meV$, $211\ meV$, and $333\ meV$. The transition energies show that long-infrared absorption/emission is obtained from the E_{32} transition as desired and the E_{21} transition has higher energy than the phonon vibrations of GaAs ($0.026\ eV$), which is crucial for heat dissipation via phonon vibration in long infrared devices.

Figure 2 shows the PDW of the quadruple QW structure under varying EF intensities. I have obtained the wave functions and corresponding energy eigenvalues for every $5\ kV/cm$ up to $80\ kV/cm$. To prevent confusion and for the sake of simplicity, we do not present every plot for different EF intensities. With the effect of EF, all three energy states are shifted up to higher energies. Localization of the ground state has also started to show up in the first and second QWs. The localization of the first excited state in the second QW is inversely proportional to EF intensity however, localization in the third QW is independent of the EF intensity. When the second excited state is localized in the fourth QW in the case of zero EF, it is mostly localized in the first and second QWs after the applied EF. In another study by Altun, wave functions and energy eigenvalues were shown for different electric fields applied to GaAs/AlGaAs QWs with periodically increasing well width. [18].

In the design, there has been no localization in the fourth QW in the case of EF but I have used the fourth QW to tune transition energies changing the QW thickness. According to the probability density functions and energy eigenvalues, $80\ kV/cm$ is the highest EF intensity. Electron leakage has started over this value and after a bit more increase, the second excited state has higher eigen energy than barrier height, which causes stopping device operation. Here I conclude that $80\ kV/cm$ is the highest EF, which can be applied to the device under consideration.

Even though there is a slight increase in E_{32} transition energy, the dipole matrix moment corresponding to the M_{32} is constant and independent from EF intensity as shown in Figure 3. This means the design shows stable operation over changing EF. Also, M_{32} is the most probable transition in the design till the highest EF intensity. E_{21} transition energy is inverse linearly proportional with EF intensity however dipole matrix element M_{21} is linearly proportional to EF intensity. Even with a decrease in E_{21}, it is higher than the phonon vibration energies of GaAs, which is the desired behavior for quantum cascade laser/detector applications. As a last, E_{31} transition is inversely proportional to EF intensity and M_{31} is decreasing at higher EF intensities, which supports radiative transition through E_{32}.

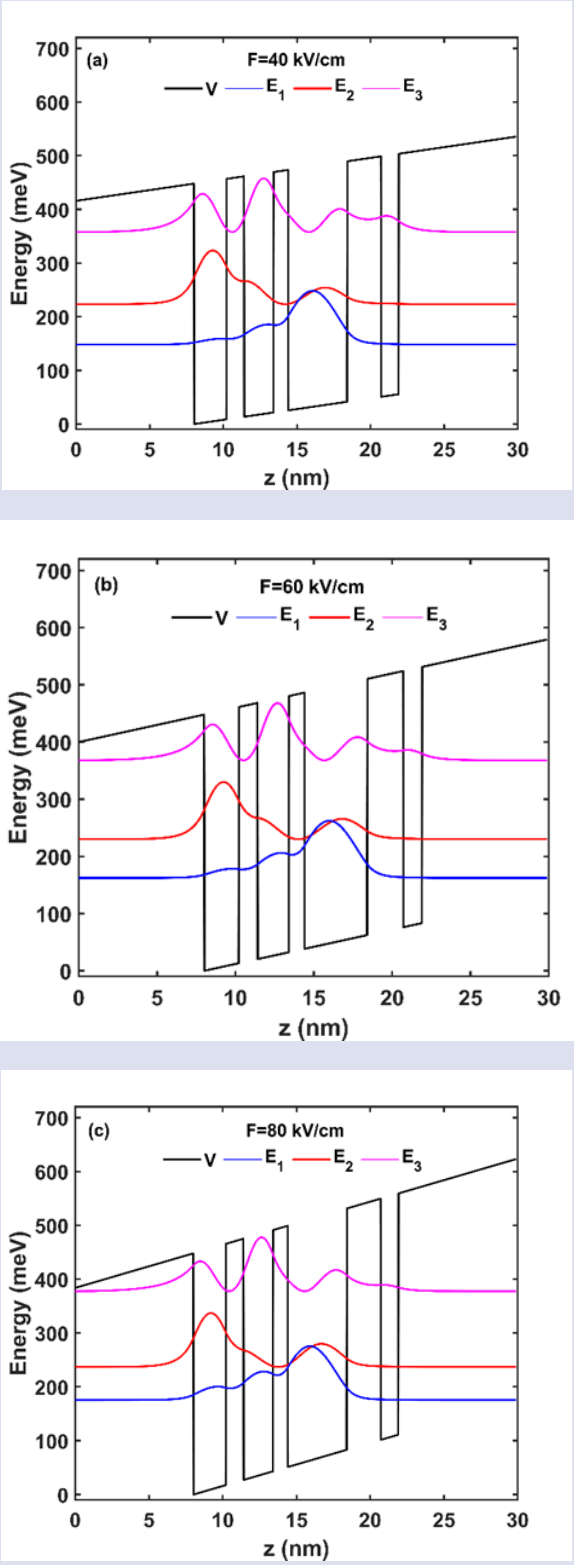

Figure 2. PDW of quadruple QW structure under varying EF intensities (a) $F = 40\ kV/cm$, (b) $F = 60\ kV/cm$, (c) $F = 80\ kV/cm$.

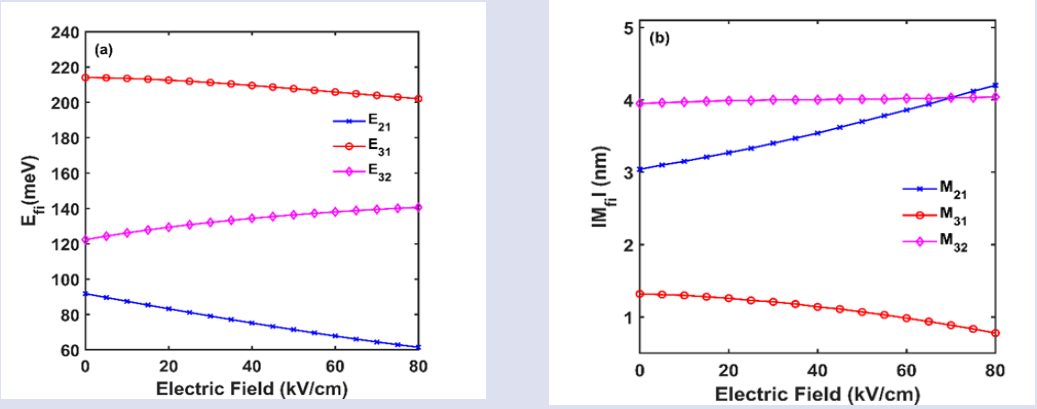

Figure 3. Transition energies and corresponding DMMEs.

In this part of the study, I have studied the effect of varying EF on absorption coefficients. In Figure 4 a-d, absorption coefficients for different EF intensities (0, 40, 60, and 80 kV/cm) and maximum values for each EF intensities are given. I have seen that the absorption coefficient of E_{21} and E_{31} transitions are factors approximately 38 and 3 lower than E_{32} when EF intensity is zero (Figure 4 a). When the EF is applied (Figure 4 a-d), the absorption coefficient of E_{21} is not changing over varying EF intensities. In total, E_{32} has shown an increasing trend while E_{31} is in a decreasing trend over EF change. This means quadruple QW structure absorbs/emits more photons under applied EF and decreases in E_{31} is an indicator of lower heat in the structure due to less absorption/emission. At the same time, the absorption coefficient of E_{21} transition is independent of the EF intensity as given in Figure 4d. This indicates that there is a constant heating effect owing to the phonon vibrations, which is independent of the increased EF and is the desired behavior for device applications. In addition, in Figure 4-d, the y-axis where the "peak of absorption coefficient" values are given is in the range of 0-9000 cm-1. Since the change of E21 is approximately in the range of 180-220 cm-1, small differences in the change on this scale cannot be seen very clearly.

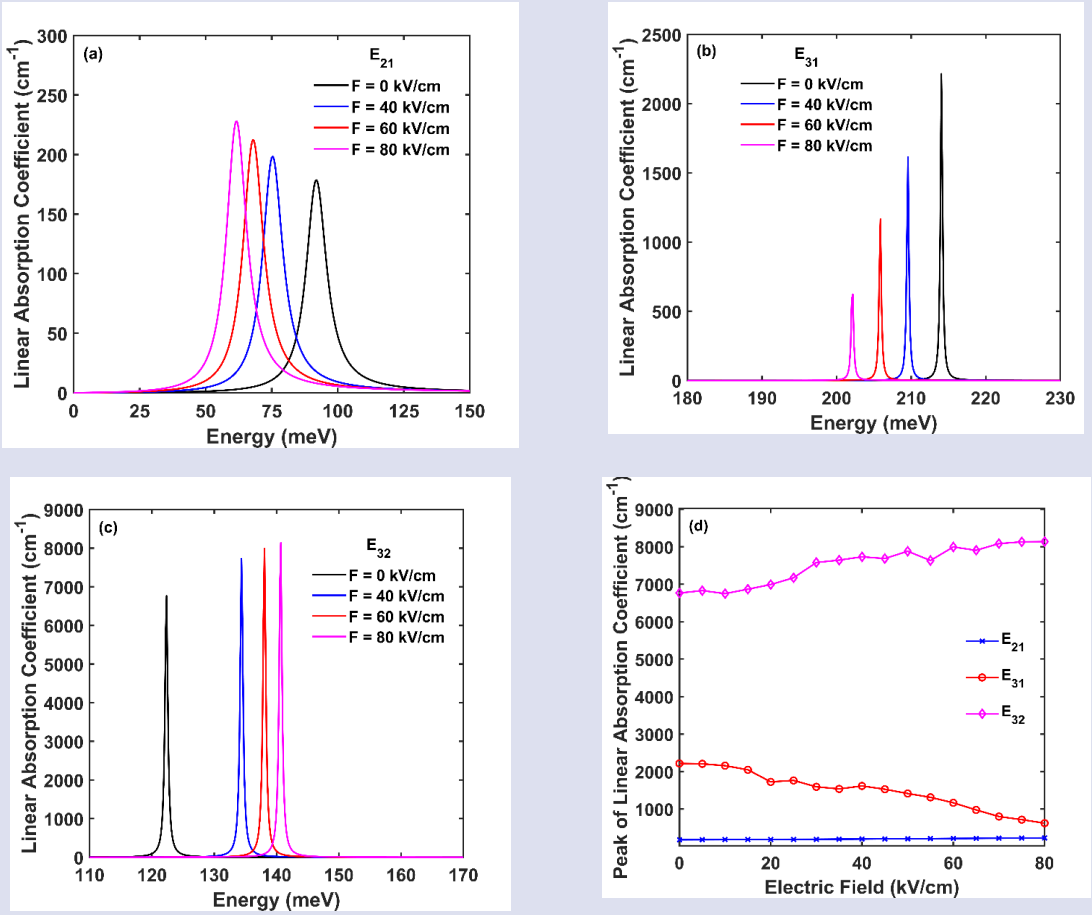

Figure 4. Absorption coefficients for F=0, F=40, F=60 and F=80 kV/cm of a) E_{21}, b) E_{31}, c) E_{32} transitions and d) maxima of absorption coefficients versus EF intensity.

In this section of the study, I have analyzed the effect of the varying EF on refractive index change. In Figure 5 a-d, refractive index change for different EF intensities (0, 40, 60, and 80 kV/cm) and maximum values for each change dependent on the EF intensities are given in Figure 5 d. The change in refractive index is inversely proportional to the EF intensity. Therefore, as seen in Figure 5 b, with the increase in EF intensity, the refractive index decreased due to dipole moments. I have observed that the linear refractive index change of E_{32} is independent of EF intensity. This is especially crucial for laser applications otherwise change in refractive index can cause a problem with waveguide and cladding layers. However, there is an incremental change in the refractive index of E_{21}, we attribute this to a decrease in transition energies and dipole matrix moment as shown in Figure 3. In addition, there is an incremental increase in refractive index change of E_{12}, this is also related to the barely increasing dipole matrix moment of E_{12} with increasing EF intensity.

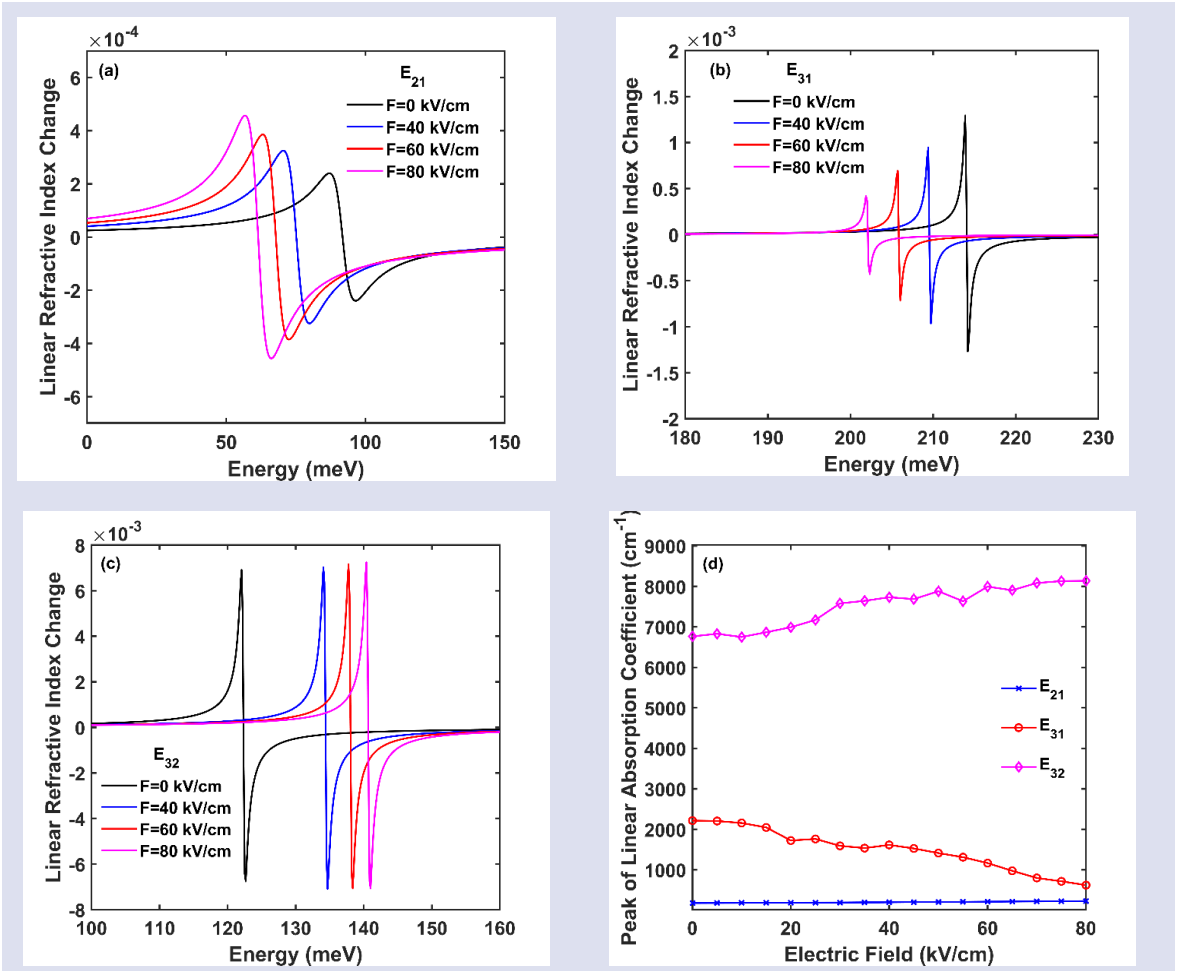

Figure 5. Linear refractive index change for F=0, F=40, F=60, and F=80 kV/cm of a) E_{21}, b) E_{31}, c) E_{32} transitions, and d) maxima of linear refractive index change versus EF intensity.

Conclusion

In the present article, I have summarized the results as follows. I have designed a quadruple QW structure to be used in long infrared devices, which emit/absorb under varying EF. To do this I have solved the Schrödinger equation using the finite element method under effective mass approximation. I have I have seen that long infrared emission/absorption can be obtained via E_{32} transition, which is between $120 - 140\ meV$. The transition energy is pretty much the same with changing EF intensities. It is observed that the overlap of the second excited state and first excited state is increasing with EF intensity due to increased localization of the second excited state in the first and second QWs. Another important parameter is the transition energy between the ground state and the first excited state, it is higher than the phonon vibration energy of GaAs. This is crucial for devices, which is operating using intraband transitions such as quantum cascade laser/detector. Linear absorption coefficients corresponding to the E_{21} and E_{31} transitions are factors 10 and 2 lower than E_{32} when EF intensity is zero. However, E_{32} has shown an increasing trend while E_{31} is in a decreasing trend over EF change while E_{21} is constant. This means there is more absorption/emission of photons via E_{32} transition. Lastly, EF intensity has a minor effect on the refractive index change, which is in total desired for semiconductor applications during the device design.

Here I show that in the quadruple QW design, a change in EF intensity does not affect the device operations. Here, I conclude that the results I have obtained show novelty in the literature and are especially important for device designs in long infrared regions.

Conflict of interests

There are no conflicts of interest in this work.

References

[1] Wang F., Slivken S., Razeghi M., High-Brightness LWIR Quantum Cascade Lasers, *Optics Letters*, 46 (20) (2021) 5193-5196.

[2] Harrer A., Schwarz B., Schuler S., Reininger P., Wirthmüller A., Detz H., MacFarland D., Zederbauer T., Andrews A. M., Rothermund M., Oppermann H., Schrenk W., Strasser G., 4.3 µm Quantum Cascade Detector in Pixel Configuration, *Optics Express*, 24 (15) (2016) 17041-17049.

[3] Vitiello M. S., Scalari G., Williams B., De Natale P., Quantum Cascade Lasers: 20 Years of Challenges, *Optics Express*, 23 (4) (2015) 5167-5182.

[4] Hanna S., Eich D., Mahlein K. M., Fick W., Schirmacher W., Thöt R., Wendler J., Figgemeier H., MCT-Based LWIR and VLWIR 2D Focal Plane Detector Arrays for Low Dark Current Applications at AIM, *Journal of Electronic Materials*, 45 (9) (2016) 4542-4551.

[5] Alaydin B. O., Ozturk E., Elagoz S., Interband Transitions Dependent on Indium Concentration in Ga1−xInxAs/GaAs Asymmetric Triple Quantum Wells, *International Journal of Modern Physics B*, 32 (05) (2017) 1850052.

[6] Hao Q., Zhao X., Tang X., Chen M., The Historical Development of Infrared Photodetection Based on Intraband Transitions, *Materials*, 16 (2023) 1562.

[7] Jiang M., Xiao H. Y., Peng S. M., Yang G. X., Liu Z. J., Zu X. T., A Comparative Study of Low Energy Radiation Response of AlAs, GaAs and GaAs/AlAs Superlattice and The Damage Effects on Their Electronic Structures, *Scientific Reports*, 8 (1) (2018) 2012.

[8] Karabulut İ., Atav Ü., Şafak H., Tomak M., Second Harmonic Generation in an Asymmetric Rectangular Quantum Well Under Hydrostatic Pressure, *Physica B: Condensed Matter*, 393 (1) (2007) 133-138.

[9] Karki H. D., Elagoz S., Baser P., The High Hydrostatic Pressure Effect on Shallow Donor Binding Energies in GaAs–(Ga, Al)As Cylindrical Quantum Well Wires at Selected Temperatures, *Physica B: Condensed Matter*, 406 (11) (2011) 2116-2120.

[10] Ozturk E., Depending on The Electric and Magnetic Field of The Linear Optical Absorption and Rectification Coefficient in Triple Quantum Well, *Optical and Quantum Electronics*, 49 (8) (2017) 270.

[11] Alaydin B. O., Effect of High Bandgap AlAs Quantum Barrier on Electronic and Optical Properties of In0.70Ga0.30As/Al0.60In0.40As Superlattice Under Applied Electric Field for Laser and Detector Applications, *International Journal of Modern Physics B*, 35 (02) (2021) 2150027.

[12] Durmuslar A. S., Billur C. A., Turkoglu A., Ungan F., Optical Properties of a GaAs Quantum Well with a New Type of Hyperbolic Confinement Potential: Effect of Structure Parameters and Intense Laser Field, *Optics Communications*, 499 (2021) 127266.

[13] Öztürk E., Sökmen İ., Resonant Peaks of The Linear Optical Absorption and Rectification Coefficients in GaAs/GaAlAs Quantum Well: Combined Effects of Intense Laser, Electric and Magnetic Fields, *International Journal of Modern Physics B,* 29 (05) (2015) 1550030.

[14] Karabulut I., Laser Field Effect on The Nonlinear Optical Properties of a Square Quantum Well Under the Applied Electric Field, *Applied Surface Science*, 256 (24) (2010) 7570-7574.

[15] Yıldırım H., Tomak M., Nonlinear Optical Properties of a Pöschl-Teller Quantum Well, *Physical Review B*, 72(11) (2005) 115340.

[16] Öztürk E., The Effects of Hydrostatic Pressure on The Nonlinear Intersubband Transitions and Refractive Index Changes of Different QW Shapes, *Optics Communications*, 285 (24) (2012) 5223-5228.

[17] Alaydin B. O., Optical Properties of GaAs/Alxga1-xas Superlattice Under E-Field for Quantum Cascade Laser Application, *Gazi University Journal of Science*, 1: (2021) 1.

[18] Altun D., Ozturk O., Alaydin B.O., Ozturk E., Linear and Nonlinear Optical Properties of a Superlattice with Periodically Increased Well Width Under Electric and Magnetic Fields, *Micro and Nanostructures*, 166 (2022) 207225.

[19] Alaydin B.O., Altun D., Ozturk O., Ozturk E., High Harmonic Generations Triggered by The Intense Laser Field in GaAs/AlxGa1-xAs Honeycomb Quantum Well Wires, *Materials Today Physics*, 38 (2023) 101232.

[20] Bai Y., Bandyopadhyay N., Tsao S., Selcuk E., Slivken S., Razeghi M., Highly Temperature Insensitive Quantum Cascade Lasers*, Appl. Phys. Lett*., 97 (2010) 251104.

[21] Alaydin B.O., Effect of High Bandgap AlAs Quantum Barrier on Electronic and Optical Properties of In0.70Ga0.30As/Al0.60In0.40As Superlattice Under Applied Electric Field for Laser and Detector Applications, *International Journal of Modern Physics B*, 35 (02) (2021) 2150027.

[22] Niculescu E. C., Eseanu N., Radu A., Heterointerface Effects on The Nonlinear Optical Rectification in a Laser-Dressed Graded Quantum Well, *Optics Communications*, 294 (2013) 276-282.

[23] Ghosh P., A., Mandal A., Sarkar S., Ghosh M., Influence of Position-Dependent Effective Mass on The Nonlinear Optical Properties of Impurity Doped Quantum Dots in Presence of Gaussian White Noise, *Optics Communications*, 367 (2016) 325-334.